Icarus 197 (2008) 585–589

Contents lists available at ScienceDirect

Icarus

www.elsevier.com/locate/icarus

First *Spitzer* observations of Neptune: Detection of new hydrocarbons

Victoria S. Meadows [a,*], Glenn Orton [b], Michael Line [c], Mao-Chang Liang [d], Yuk L. Yung [d], Jeffrey Van Cleve [e], Martin J. Burgdorf [f]

[a] *Spitzer Science Center/California Institute of Technology, MS 220-6, 1200 E. California Blvd, Pasadena, CA 91125, USA*
[b] *Jet Propulsion Laboratory/California Institute of Technology, MS 169-237, 4800 Oak Grove Drive, Pasadena, CA 91109, USA*
[c] *University of Wisconsin, Department of Astronomy, 5534 Sterling Hall, 475 N. Charter St., Madison, WI 53706, USA*
[d] *California Institute of Technology, Geological and Planetary Sciences, 1200 E. California Blvd, Pasadena, CA 91125, USA*
[e] *Ball Aerospace and Technologies Corp., 1600 Commerce St., Boulder, CO 80301, USA*
[f] *Astrophysics Research Institute, Liverpool John Moores University, Twelve Quays House, Egerton Wharf, Birkenhead, CH41 1LD, UK*

ARTICLE INFO

Article history:
Received 14 November 2007
Revised 19 May 2008
Available online 20 June 2008

Keywords:
Neptune, atmosphere
Spectroscopy
Infrared observations
Atmospheres, composition

ABSTRACT

We present the first spectra of Neptune taken with the *Spitzer* Space Telescope, highlighting the high-sensitivity, moderate-resolution 10–20 μm (500–1000 cm^{-1}) spectra. We report the discovery of methylacetylene (CH_3C_2H) and diacetylene (C_4H_2) with derived 0.1-mbar volume mixing ratios of $(1.2 \pm 0.1) \times 10^{-10}$ and $(3 \pm 1) \times 10^{-12}$ respectively.

1. Introduction

Neptune's atmosphere is primarily composed of hydrogen, helium and methane. However, spectroscopy of the planet to date has revealed many higher-order hydrocarbons, the products of reactions that are initiated by the photodissociation of CH_4. Ground-based mid-infrared (MIR) spectroscopy first detected CH_4, C_2H_6, and C_2H_2, and provided tentative evidence for CH_3D and C_2H_4 in the Neptune stratosphere (Orton et al., 1987, and references therein), while ground-based millimeter-wave observations first detected HCN (Marten et al., 1993). The first firm detection of C_2H_4 at 10.55 μm (948 cm^{-1}) was provided by the Infrared Space Observatory (ISO)/PHT-S (Schultz et al., 1999). Voyager observations confirmed the ground-based detection of C_2H_2 (Conrath et al., 1989; Bézard et al., 1991; Bishop et al., 1995) and ISO observations first revealed the CH_3 radical (Bézard et al., 1999). Detecting and quantifying these trace hydrocarbons provides crucial constraints for photochemical models of the Neptune atmosphere, which seek to explain and predict species abundances via the balance between chemical production and destruction rates, and loss to the lower atmosphere by condensation and eddy diffusion (Bishop et al., 1995; Moses et al., 2005). In addition to hydrocarbons, Neptune and the other Jovian planets are known to harbor oxygen-bearing compounds, including CO (Marten et al., 1993) and H_2O and CO_2 (Moses, 1992; Feuchtgruber et al., 1997; Moses et al., 2000). While Neptune's CO likely has an internal source, in addition to an external one (Lellouch et al., 2005; Hesman et al., 2007) the presence of water in the stratospheres of the Jovian planets above their condensation levels implies an external source, most likely from interplanetary micrometeorites (Feuchtgruber et al., 1997).

To provide further constraints for models of Neptune's atmosphere and to continue the search for both higher-order hydrocarbons and oxygen-bearing compounds, we used the InfraRed Spectrograph (IRS) on board the *Spitzer* Space Telescope, which provides two orders of magnitude more sensitivity than previous missions.

2. Observations

All spectra were taken with the InfraRed Spectrograph (IRS; Houck et al., 2004) on the *Spitzer* Space Telescope (Werner et al., 2004). A set of three 20-min duration disk-averaged observations of Neptune, spanning wavelengths from 5.2 to 38 μm (263–1923 cm^{-1}), were initiated at UTC 2004-05-15 00:58, 06:17, and 12:12. This observing pattern centered on roughly evenly spaced longitudes on Neptune, thereby covering the entire globe. The observations presented here highlight the Short-High (SH) module of the IRS, spanning 9.9–19.6 μm (510–1010 cm^{-1}), with a spectral resolution $R = \lambda/\Delta\lambda \sim 600$. A spectrum from order 2 of the Short-Low (SL) module which spans 5.2–8.7 μm (1149–1923 cm^{-1})

* Corresponding author. Now at The University of Washington, Department of Astronomy, Box 351580, Seattle, WA 98195, USA.
E-mail address: vsm@astro.washington.edu (V.S. Meadows).

0019-1035/$ – see front matter
doi:10.1016/j.icarus.2008.05.023

with a spectral resolution of $R = \lambda/\Delta\lambda \sim 120$ is also shown. The 2.28″ equatorial diameter planet was nodded in the long dimension within the 4.7″ × 11.3″ slit. The total exposure time for the SH data, combining both slit positions, was 100 s on source per Neptune longitude, so 300 s total for the majority of the spectra shown here, and 50 s on source per Neptune longitude, or 150 s for all longitudes, for the SL spectrum.

3. Data analysis

The IRS SH observations were reduced using the Spitzer data processing pipeline to remove instrumental artifacts. The resulting 2-D Post Basic Calibrated Data (PBCD) have all cycles coadded for a given nod position. For the analysis presented here, data at all three longitudes were coadded to improve S/N. Primarily to remove the zodiacal light contribution, the spectra were then sky-subtracted using the *Spitzer* IRS Custom Extractor (SPICE) spectroscopy reduction software (http://ssc.spitzer.caltech.edu/postbcd/spice.html), and a *Spitzer* high-resolution sky spectrum taken at the same ecliptic latitude as Neptune, but from a subsequent observing campaign (UTC 2005-11-22 00:47). 1-D spectra were extracted from the 2-D sky-subtracted spectral images using SPICE. SPICE also provided the flux calibration for the data from a set of standard stars that were observed within the same spacecraft instrument campaign. IRS absolute calibration for point sources is believed to be accurate to within 10% (3σ). For the Short-Low data, the analysis was identical, with the exception that sky subtraction was performed using sky observations taken simultaneously with the planetary data.

The brightness temperatures were derived from radiances, with a planetary equatorial diameter of 2.28″ as viewed from *Spitzer* on the date of observation (corresponding to a solid angle of 9.6×10^{-11} sterad), obtained from the JPL Horizons ephemeris system.

4. The atmospheric model

To confirm new identifications and determine mixing ratios, disk-averaged synthetic spectra were generated for comparison with the data. We used a radiative transfer program which integrates over the disk of the planet in a 5-stream upwelling model using curvilinear geometry. The average upwelling radiance is obtained by using Gaussian quadrature in the cosine of the emission angle to integrate over the disk. The temperature structure adopted for the model is taken from Moses et al. (2005) and is consistent with that of Feuchtgruber et al. (1999). As a validation, we determined that this profile was consistent with our *Spitzer* measurement of the 17.04 μm (587 cm^{-1}) S(1) H_2 quadrupole line, which is sensitive to the stratospheric temperature profile. We note that we did not correct for variability in the *para*-H_2/*ortho*-H_2 ratio (Fouchet et al., 2003); as the spectral resolution of the data ($R = 600$) significantly precludes sensitivity to this ratio. The initial vertical profiles for the atmospheric constituent mixing ratios were taken from Neptune Model A of Moses et al. (2005) that has generally provided best fits to previous ground and space-based observations. Spectroscopic line parameters for each constituent were obtained from the GEISA databank (Jacquinet-Husson et al., 2004, 1999, and references therein). Absorption cross-sections from the PNNL database (Sharpe et al., 2004) were used for CH_3COOH. The H_2 collision-induced opacity was calculated following Birnbaum et al. (1996).

5. Results

Both our SL and SH spectra contain many features belonging to previously discovered constituents of Neptune's atmosphere, including CH_4, CH_3D, C_2H_2, and C_2H_6 (e.g. Orton et al., 1987, and references therein), H_2O and CO_2 (Feuchtgruber et al., 1997), C_2H_4 (Schultz et al., 1999), and the CH_3 radical (Bézard et al., 1999). Excerpts of the spectra that include features from C_2H_6, CO_2, CH_4 and CH_3 are shown in Fig. 1.

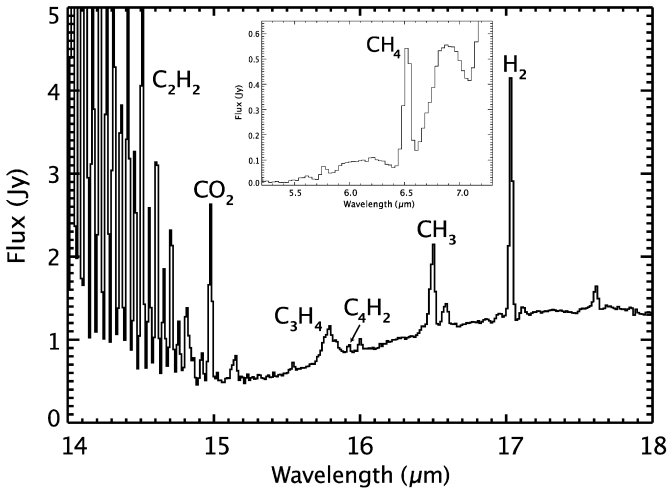

Fig. 1. Selected regions of the Spitzer SH coadded spectrum and an insert of part of the SL spectrum showing the previously detected species, CH_4, C_2H_2, CO_2, CH_3 and H_2, and the newly discovered species, CH_3C_2H and C_4H_2. Features with no identification at the time of submission of this paper can be seen at 15.15 μm (660 cm^{-1}), 15.55 μm (643 cm^{-1}), 16.00 μm (625 cm^{-1}) and 17.62 μm (568 cm^{-1}).

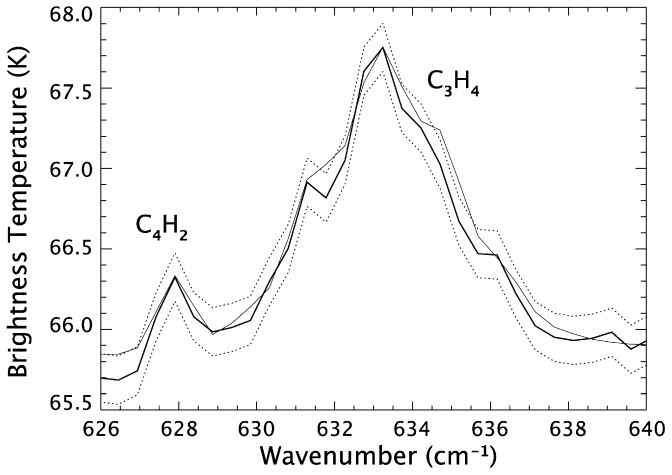

Fig. 2. Portion of the Spitzer SH Neptune spectrum, converted to brightness temperature, showing two features identified as diacetylene (C_4H_2) and methylacetylene (CH_3C_2H). Data are indicated by the thick solid line, which is surrounded by dotted lines representing the range of the spectrum within ±1 standard deviation in the measurements. The thin solid line represents the best fit of a model to the data.

Our observations are generally consistent with previous spectra and, thus, the measured strengths of the relevant bands. For example, the *Spitzer* CO_2 feature was fit using a scaling of Moses et al. (2005) model to derive a volume mixing ratio of 7.8×10^{-10} at a pressure level of 0.1 mbars. This is comparable to the mixing ratio for CO_2 derived from ISO measurements of Neptune, that was found to be 5×10^{-10}, assuming a vertically uniform mixing ratio above a condensation level of 5.5 mbar (Feuchtgruber et al., 1997).

These first *Spitzer* spectra reveal several new constituents. Fig. 2 shows an excerpt of the spectrum containing two of these, which we identify as belonging to the ν_9 band of methylacetylene (CH_3C_2H) at 15.8 μm (633 cm^{-1}) and the ν_8 band of diacetylene (C_4H_2) at 15.92 μm (628 cm^{-1}). The diacetylene feature is detected at the 3σ level and the methylacetylene feature is detected at the 12σ level of confidence.

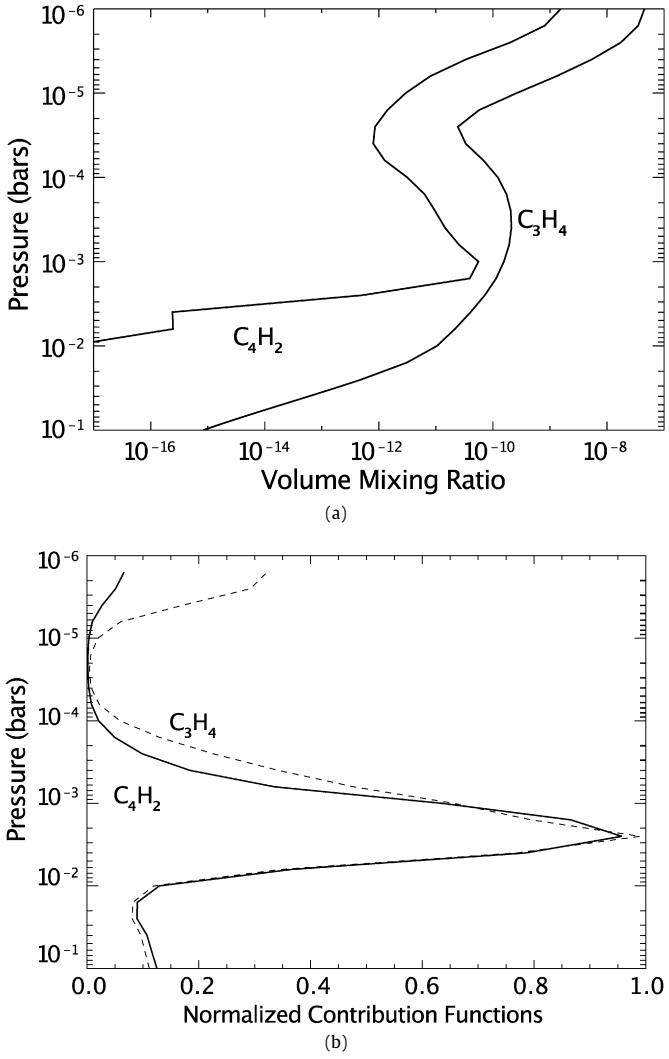

Fig. 3. (a) Vertical profiles of diacetylene (C_4H_2) and methylacetylene (CH_3C_2H) which provide the best fit to the data. The profiles were derived by scaling the abundances in Moses et al. (2005) Neptune model A to achieve a best fit. If constant mixing ratios in the stratosphere are assumed instead, the best fitting volume mixing ratios for C_4H_2 and CH_3C_2H are $2.7 \pm 0.8 \times 10^{-11}$ and $2.1 \pm 0.2 \times 10^{-10}$, respectively. (b) Normalized contribution functions for C_4H_2 and CH_3C_2H at the wavelengths of observation, showing sensitivity to both constituents near the same atmospheric vertical levels.

To fit the observed features to verify their identity and calculate abundances, we assumed vertical distributions for C_4H_2 and CH_3C_2H based on those for Neptune Model A published by Moses et al. (2005). The values for the abundances were subsequently scaled uniformly at all altitudes until a best fit was obtained. We are sensitive to radiance emitted from a broad vertical region between 0.1 and 10 mbar for both constituents. For our adopted temperature structure, the scaled constituent vertical profiles which best fit the data are shown in Fig. 3. This figure also describes the best fit inferred abundances for vertically uniform profiles. For CH_3C_2H, the best fit scaling factor is 1.2 ± 0.1 times that of Neptune Model A (Moses et al., 2005). However, for C_4H_2 the best fit scaling factor is 13.5 times that in Model A, with an uncertainty range of 8.5 to 16.5 as derived from the observed spectral measurement errors.

The *Spitzer* spectra also presented many previously unidentified features. Several of these can be seen in Fig. 1 at 15.08 μm (663 cm^{-1}), 15.15 μm (660 cm^{-1}), 15.55 μm (643 cm^{-1}) and 16.01 μm (624.5 cm^{-1}). We attempted to fit several of these features with compounds that had close features in line lists, including HC_3N for the 15.08 μm (663 cm^{-1}) feature, acetic acid (CH_3COOH) for the 15.55 μm (643 cm^{-1}) feature, and formic acid (HCOOH) or triacetylene (C_6H_2) for the 16.01 μm (624.5 cm^{-1}) feature. But in all attempts the known line parameters were close, but did not produce a sufficiently good fit to the wavelength position in the *Spitzer* data. We note however that the modeled CO_2 band at 14.98 μm (667 cm^{-1}) was a good fit to the *Spitzer* data, so it is unlikely that the discrepancy between the observed *Spitzer* unidentified lines and the models are due to data wavelength calibration errors. We also explored the possibility of the feature longward of the CH_3 radical Q-branch at 16.48 μm (607 cm^{-1}) being attributable to furan (C_4H_4O), as this molecule has its ν_{21} fundamental at 16.58 μm (603 cm^{-1}). However, subsequent modeling revealed that both of the features at 16.48 and 16.58 μm could be attributed solely to the CH_3 radical.

6. Discussion

CH_3C_2H and C_4H_2 are stable molecules yet involved in a myriad of photochemical reactions believed to be common to giant planet atmospheres. C_4H_2 formation is strongly sensitive to C_2H_2 photolysis, whereas CH_3C_2H formation has sources that depend in part on both C_2H_2 and C_2H_6 (Moses et al., 2005). Their detection and quantification on Neptune provide the first probe of C_3H_x and C_4H_x related chemistry on this planet, and important new constraints for photochemical models of the stratospheres of the giant planets. With prior results for Jupiter, Saturn and Titan (Encrenaz et al., 1999; Fouchet et al., 2000; Kunde et al., 2004; Flasar et al., 2005; Kunde et al., 1981; Hanel et al., 1981), and recent *Spitzer* results for Uranus (Burgdorf et al., 2006), methylacetylene and diacetylene have now been detected and quantified on all four giant planets and Titan.

Our results show good agreement between the model predictions and the data for methylacetylene abundance. However, the diacetylene observations suggest an abundance that is an order of magnitude greater than the model predicts. The resulting measured ratio of CH_3C_2H/C_4H_2 is in the range 2 to 4, compared to the model prediction of ~ 33. Even if we conservatively adopted the warmest temperature profile of Marten et al. (2005), warmer than the hottest profile adopted by Hesman et al. (2007)—the volume mixing ratio of C_4H_2 predicted by Moses et al. (2005) still needs to be scaled upward by a factor of 3.4 to match our data. Adopting this temperature profile then requires the Moses et al. (2005) profile of CH_3C_2H to be scaled downward using a factor of 0.95. The relative profiles of the two constituents are sufficiently similar so that changes of the assumed temperature profile will influence the scaling for both constituents more or less similarly. Our tests show that the inconsistency of the measured to predicted ratio of these two constituents is also true if we assume a uniform distribution with altitude.

Similarly, *Spitzer* IRS observations for Uranus also inferred a measured CH_3C_2H/C_4H_2 ratio in the range of 3 to 5 (Burgdorf et al., 2006) vs the best available model that includes CH_3C_2H condensation and predicts a ratio of ~20 (Julie Moses, private communication). Measured CH_3C_2H/C_4H_2 ratios for Saturn and Jupiter are much larger, however, being 10 and >20 respectively, and are well matched by the model predictions. We note also that the Neptune diacetylene, although in a similar abundance ratio with methylacetylene to that observed in the *Spitzer* Uranus data, is nonetheless a relatively weak spectral feature in comparison. This is likely due to the interplay between the vertical distribution of these species and the modeled planetary temperature structure. Neptune's relatively isothermal stratosphere would result in a less pronounced emission feature compared to the constant rise in temperature inferred for the similar region in the Uranus atmosphere.

Based on this preliminary dataset, it is not yet clear whether the discrepancy between the data and the model predictions for diacetylene is a systematic one, or subject to temporal variability in this constituent abundance and distribution. The issue of whether or not there is constituent temporal variability will be addressed with a more comprehensive dataset in a subsequent paper.

However, if subsequent observations and analyses confirm that the diacetylene is detected in abundances systematically higher than the model predictions, then this observation, combined with the relatively good fits for both methylacetylene and acetylene could point to a physical, rather than chemical discrepancy with the current models. The measured column abundance for C_4H_2 is largely controlled by the pressure level at which the C_4H_2 condenses and the model discrepancy may therefore be in the predicted condensation level, rather than solely in the modeled chemistry. Both temperature profile and vapor pressure uncertainties could be contributing to errors in the condensation level predictions. The observations discussed here and subsequent observations will help us to constrain where C_4H_2 is condensing and help in the development of improved models for C_3H_x and C_4H_x chemistry for the ice giants.

7. Conclusion

Spitzer's enhanced sensitivity has enabled us to discover and derive preliminary abundances for two hydrocarbons, methylacetylene and diacetylene, on Neptune. Assuming a temperature profile consistent with the size of the quadrupole of well mixed H_2, the abundance of methylacetylene matches that expected in the theoretical profiles of Moses et al. (2005). The same cannot be said for diacetylene which is present at significantly higher abundances than those computed in the same model. This conclusion is bolstered by the fact that we are sensitive to both constituents near the same vertical levels, and their abundance ratio, which is not sensitive to the assumed temperature profile, is inconsistent with the model. This conclusion is true either if we scale the vertical abundance profiles in the model to fit the observed emission or if we assume a constant vertical mixing ratio.

Acknowledgments

This work is based on observations made with the *Spitzer* Space Telescope, which is operated by the Jet Propulsion Laboratory, California Institute of Technology under a contract with NASA. M.C.L. and Y.L.Y. were supported in part by NASA Grant NAG5-13296 to the California Institute of Technology. We wish to thank Julianne Moses for her model vertical constituent profiles in advance of publication—and for several extremely helpful discussions. The IRS was a collaborative venture between Cornell University and Ball Aerospace Corporation funded by NASA through the Jet Propulsion Laboratory and Ames Research Center.

References

Bézard, B., Romani, P.N., Conrath, B.J., Maguire, W.C., 1991. Hydrocarbons in Neptune's stratosphere from Voyager infrared observations. J. Geophys. Res. Suppl. 96, 18961–18975.

Bézard, B., Romani, P.N., Feuchtgruber, H., Encrenaz, T., 1999. Detection of the methyl radical in Neptune. Astrophys. J. 515, 868–872.

Birnbaum, G., Borysow, A., Orton, G.S., 1996. Collision-induced absorption of H_2–H_2 and H_2–He in the rotational and fundamental band for planetary applications. Icarus 123, 4–22.

Bishop, J., Atreya, S.K., Romani, P.N., Orton, G.S., Sandel, B.R., Yelle, R.V., 1995. The middle and upper atmosphere of Neptune. In: Cruickshank, D.P. (Ed.), Neptune and Triton. University of Arizona Press, Tucson, pp. 427–487.

Burgdorf, M., Orton, G., van Cleve, J., Meadows, V., Houck, J., 2006. Detection of new hydrocarbons in Uranus' atmosphere by infrared spectroscopy. Icarus 184, 634–637.

Conrath, B., Flasar, F.M., Hanel, R., Kunde, V., Maguire, W., Pearl, J., Pirraglia, J., Samuelson, R., Cruikshank, D., Horn, L., 1989. Infrared observations of the neptunian system. Science 246, 1454–1459.

Encrenaz, T., Drossart, P., Feuchtgruber, H., Lellouch, E., Bézard, B., Foucet, T., Atreya, S.K., 1999. The atmospheric composition and structure of Jupiter and Saturn from ISO observations: A preliminary review. Planet. Space Sci. 47, 1225–1242.

Feuchtgruber, H., Lellouch, E., de Graauw, T., Bézard, B., Encrenaz, T., Griffin, M., 1997. External supply of oxygen to the atmospheres of the giant planets. Nature 389, 159–162.

Feuchtgruber, H., Lellouch, E., Encrenaz, T., de Graauw, T., Davis, G.R., 1999. Detection of HD in the atmospheres of Uranus and Neptune: A new determination of the D/H ratio. Astron. Astrophys. 341, L17–L21.

Flasar, F.M., Achterberg, R.K., Conrath, B.J., Bjoraker, G.L., Jennings, D.E., Pearl, J.C., Romani, P.N., Simon-Miller, A.A., Kunde, V.G., Nixon, C.N., Bézard, B., Orton, G.S., Spilker, L.J., Irwin, P.G.J., Teanby, N.A., Spencer, J.A., Owen, T.C., Brasunas, J., Segura, M.E., Carlson, R., Mamoutkine, A., Gierasch, P.J., Schinder, P.J., Ferrari, C., Showalter, M.R., Barucci, A., Courtin, R., Coustenis, A., Fouchet, T., Gautier, D., Lellouch, E., Marten, A., Prangé, R., Strobel, D.F., Calcutt, S.B., Read, P.L., Taylor, F.W., Bowles, N., Samuelson, R.E., Abbas, M.M., Raulin, F., Ade, P., Edgington, S., Pilorz, S., Wallis, B., Wishnow, E., 2005. Temperatures, winds, and composition in the Saturn system. Science 307, 1247–1251.

Fouchet, T., Lellouch, E., Bézard, B., Feuchtgruber, H., Drossart, P., Encrenaz, T., 2000. Jupiter's hydrocarbons observed with ISO-SWS: Vertical profiles of C_2H_6 and C_2H_2, detection of CH_3C_2H. Astron. Astrophys. 355, L13–L17.

Fouchet, T., Lellouch, E., Feuchgruber, H., 2003. The hydrogen *ortho*-to-*para* ratio in the stratospheres of the giant planets. Icarus 161, 127–143.

Hanel, R., Conrath, B., Flasar, F.M., Kunde, V., Maguire, W., Pearl, J.C., Pirraglia, J., Samuelson, R., Herath, L., Allison, M., Cruikshank, D.P., Gautier, D., Gierasch, P.J., Horn, L., Koppany, R., Ponnamperuma, C., 1981. Infrared observations of the saturnian system from Voyager 1. Science 212, 192–200.

Hesman, B.E., Davis, G.R., Matthews, H.E., Orton, G.S., 2007. The abundance profile of CO in Neptune's atmosphere. Icarus 186, 342–353.

Houck, J., Roellig, T., van Cleve, J., Forrest, W., Herter, T., Lawrence, C., Matthews, K., Reitsema, H., Soifer, B., Watson, D., Weedman, D., Huisjen, M., Troeltzsch, J., Barry, D., Bernard-Salas, J., Blacken, C., Brandl, B., Charmandaris, V., Devost, D., Gull, G., Hall, P., Henderson, C., Higdon, S., Pirger, B., Schoenwald, J., Sloan, G., Uchida, K., Appleton, P., Armus, L., Burgdorf, M., Fajardo-Acosta, S., Grillmair, C., Ingalls, J., Morris, P., Teplitz, H., 2004. The infrared spectrograph on the *Spitzer* space telescope. Astrophys. J. Suppl. 154, 18–24.

Jacquinet-Husson N.E., and the LMD Team, 2004. The 2003 edition of GEISA: A spectroscopic database system for the second generation vertical sounders radiance simulation. In: 35th COSPAR Scientific Assembly, No. 2521.

Jacquinet-Husson, N., Arie, E., Barbe, A., Brown, L.R., Bonnet, B., Camy-Peyret, C., Champion, J.-P., Chedin, A., Chursin, A., Clerbaux, C., Duxbury, G., Flaud, J.-M., Fourrie, N., Fayt, A., Graner, G., Gamache, R.R., Goldman, A., Guelachvili, G., Hartmann, J.M., Hilco, J.C., Lefevre, G., Naumenko, V., Nikitin, A., Perrin, A., Reuter, D., Rosenmann, L., Rothman, L.S., Scott, N.A., Selby, J., Sinitsa, L.N., Sirota, J.M., Smith, A., Smith, K., Tyuterevi, Vi.G., Tipping, R.H., Urban, S., Varanasi, P., Weber, M., 1999. The 1997 spectroscopic GEISA databank. J. Quant. Spectrosc. Radiat. Trans. 62, 205–254.

Kunde, V.G., Aikin, A.C., Hanel, R.A., Jennings, D.E., Maguire, W.C., Samuelson, R.E., 1981. C_4H_2, HC_3N and C_2N_2 in Titan's atmosphere. Nature 292, 686–688.

Kunde, V.G., Flasar, F.M., Jennings, D.E., Bézard, B., Strobel, D.F., Conrath, B.J., Nixon, C.A., Bjoraker, G.L., Romani, P.N., Achterberg, R.K., Simon-Miller, A.A., Irwin, P., Brasunas, J.C., Pearl, J.C., Smith, M.D., Orton, G.S., Gierasch, P.J., Spilker, L.J., Carlson, R.C., Mamoutkine, A.A., Calcutt, S.B., Read, P.L., Taylor, F.W., Fouchet, T., Parrish, P., Barucci, A., Courtin, R., Coustenis, A., Gautier, D., Lellouch, E., Marten, A., Prangé, R., Biraud, Y., Ferrari, C., Owen, T.C., Abbas, M.M., Samuelson, R.E., Raulin, F., Ade, P., Césarsky, C.J., Grossman, K.U., Coradini, A., 2004. Jupiter's atmospheric composition from the Cassini thermal infrared spectroscopy experiment. Science 305, 1582–1587.

Lellouch, E., Moreno, R., Paubert, G., 2005. A dual origin for Neptune's carbon monoxide? Astron. Astrophys. 430, L37–L40.

Marten, A., Gautier, D., Owen, T., Sanders, D.B., Matthews, H., Atreya, S.K., Tilanus, R.P.J., Deane, J.R., 1993. First observations of CO and HCN on Neptune and Uranus at millimeter wavelengths and the implications for atmospheric chemistry. Astrophys. J. 406, 285–297.

Marten, A., Matthews, H.E., Owen, T., Moreno, R., Hidayat, T., Biraud, Y., 2005. Improved constraints on Neptune's atmosphere from submillimetre-wavelength observations. Astron. Astrophys. 429, 1097–1105.

Moses, J.I., 1992. Meteoroid ablation in Neptune's atmosphere. Icarus 99, 368–383.

Moses, J.I., Lellouch, E., Bézard, B., Gladstone, G.R., Feuchtgruber, H., Allen, M., 2000. Photochemistry of Saturn's atmosphere. II. Effects of an influx of external material. Icarus 145, 166–202.

Moses, J.I., Fouchet, T., Bézard, B., Gladstone, G.R., Lellouch, E., Feuchtgruber, H., 2005. Photochemistry and diffusion in Jupiter's stratosphere: Constraints from ISO observations and comparisons with other giant planets. J. Geophys. Res. 110, doi:10.1029/2005JE002411. E08001.

Orton, G., Aitken, D., Roche, P., Smith, C., Caldwell, J., Snyder, R., 1987. The spectra of Uranus and Neptune at 7–14 and 17–23 μm. Icarus 70, 1–12.

Schultz, B., Encrenaz, T., Bézard, B., Romani, P.N., Lellouch, E., Atreya, S.K., 1999. Detection of C_2H_4 in Neptune from ISO/PHT-S observations. Astron. Astrophys. 350, L13–L17.

Sharpe, Steven W., Johnson, Timothy J., Sams, Robert L., Chu, Pamela M., Rhoderick, George C., Johnson, Patricia A., 2004. Gas-phase databases for quantitative infrared spectroscopy. Appl. Spectrosc. 58, 1452–1461.

Werner, M., Roellig, T., Low, F., Rieke, G., Rieke, M., Hoffmann, W., Young, E., Houck, J., Brandl, B., Fazio, G., Hora, J., Gehrz, R., Helou, G., Soifer, B., Stauffer, J., Keene, J., Eisenhardt, P., Gallagher, D., Gautier, T., Irace, W., Lawrence, C., Simmons, L., Van Cleve, J., Jura, M., Wright, E., 2004. The Spitzer Space Telescope Mission. Astrophys. J. Suppl. 154, 1–9.